RSC Advances

PAPER

Check for updates

Dual-wavelength synchronously mode-locked Nd:LaGGG laser operating at 1.3 μm with a SESAM

Xiaoli Sun, [a] Jingliang He,[*a] Zhitai Jia, [*a] Jian Ning,[a] Ruwei Zhao,[a] Xiancui Su,[a] Yiran Wang,[a] Baitao Zhang,[a] Kejian Yang[b] and Shuang Zhao[c]

We have demonstrated a diode-end-pumped synchronously dual-wavelength mode-locked Nd^{3+}:$(La_{0.1}Gd_{0.9})_3Ga_5O_{12}$ (Nd:LaGGG) laser operating at 1.3 μm with a semiconductor saturable absorber mirror (SESAM) for the first time to our knowledge. The mode-locked laser emitted an average output power of 530 mW with two wavelengths centered at 1331.2 and 1336.5 nm. The pulse duration and repetition rate were 17 ps and 37.6 MHz, respectively. A frequency beat signal with respect to two stationary wave interference patterns of 0.876 THz was observed from the autocorrelation trace.

Introduction

Picosecond solid-state lasers at 1.3 μm are attractive for applications such as remote sensing, information storage, atmospheric pollution monitoring, and so on.[1] It is also important for efficient fiber communication due to the coincidence with low-dispersion and low-loss. The efficient way to acquire 1.3 μm picosecond lasers is by mode-locking Nd^{3+}-doped lasers related to the $^4F_{3/2} \rightarrow ^4I_{13/2}$ transitions.[2] To ensure the 1.3 μm mode-locking laser performance, two key points should be considered. One is the choice of the saturable absorber at 1.3 μm. The parameters such as modulation depth, recovery time and non-saturable loss play an important role in building mode-locked pulses. As a kind of promising saturable absorber, semiconductor saturable absorber mirrors (SESAMs) have been proven to be a highly efficient and stable mode-locker due to their inherent simplicity and reliable operation.[3–5] Another is the choice of gain mediums. Factors such as the emission bandwidths influence the mode-locked pulse characteristics much. As a derivative of Nd^{3+}:$Gd_3Ga_5O_{12}$ (Nd:GGG) crystal, Nd^{3+}:$(La_{0.1}Gd_{0.9})_3Ga_5O_{12}$ (Nd:LaGGG) not only has the similar properties with Nd:GGG such as good thermal properties,[6–9] but possesses the wider inhomogeneous broadened emission spectra due to the fact that a part of Gd^{3+} ions is substituted with La^{3+} in the crystal. Thus it offers an opportunity for Nd^{3+} and the substitutive ions to enter 24c and 16a sites, which contributes to the more disordered structure. Each active ion is located in the nonequivalent ligand field, resulting in the multi-center distributions of Nd^{3+} ions and subsequently broadening

the emission spectra.[9] As Fu et al. have reported, the Nd^{3+} segregation coefficient of Nd:LaGGG is higher than that of Nd:GGG because La^{3+} ion has a larger radius (106.1 pm) than that of Gd^{3+} ion (93.8 pm).[9,10] Moreover, Nd:LaGGG crystal has a good thermal performance (the thermal conductivity of 4.76 W m^{-1} K^{-1} under room temperature). Up to now, the passively Q-switched Nd:LaGGG laser at 1.3 μm has been demonstrated, with the output power of 1.1 W and the pulse width of 27.54 ns.[11] However, no work on mode-locking operation of Nd:LaGGG crystal at 1.3 μm has been reported yet.

Dual-wavelength synchronously mode-locked ultra-short laser has great contribution to the applications such as nonlinear frequency conversion and terahertz radiation.[12–14] Nd^{3+}-doped laser crystals, because of the relatively strong splitting of Stark levels on $^4F_{3/2} \rightarrow ^4I_{13/2}$ transition, are regarded as suitable gain media for the dual-wavelength generation.[2,15] The fluorescence spectrum of Nd:LaGGG crystal indicates its gain spectra have multiple closely spaced, but well defined spectral bands. Under appropriate experimental conditions, one or more of these gain spectral bands can be mode locked, resulting in the multi-wavelength mode locking of the lasers.[9] However, the strong gain competition between each emission line is the crucial problem to generate stable simultaneously multi-wavelength mode-locked laser pulses.[16]

In this paper, we have demonstrated a dual-wavelength synchronously mode-locked Nd:LaGGG laser centered at 1331.2 nm and 1336.5 nm. An average output power of 530 mW was obtained with the pulse width of 17 ps and the repetition rate of 37.6 MHz, corresponding to single pulse energy of 14.09 nJ and a peak power of 828.57 W. Interference pattern with beating period of 1.14 ps was found in the autocorrelation trace of the mode-locked pulse, corresponding to beat frequency value of 0.876 THz, which indicated the potential of such dual-wavelength mode-locked Nd:LaGGG laser in generating THz radiations.

[a] The State Key Laboratory of Crystal Materials, Shandong University, Jinan 250100, China. E-mail: jlhe@sdu.edu.cn; z.jia@sdu.edu.cn

[b] The School of Information Science and Engineering, Shandong University, Jinan 250100, China

[c] The College of Physical Science and Technology, Jinan University, Jinan 250022, China
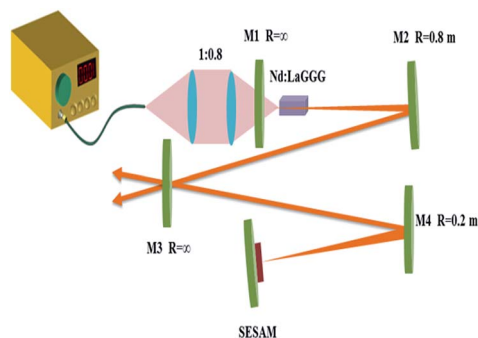
Fig. 1 Schematic of the dual-wavelength mode-locked Nd:LaGGG laser.

Fig. 2 (a) Average output power *versus* absorbed pump power. (b) The mode-locked pulse train recorded with time span of 50 ns per div and 1 ms per div.

Experimental setup

As schematically shown in Fig. 1, the dual-wavelength mode-locked Nd:LaGGG laser was realized in a 4.1 m-long resonator. The pump source was an 808 nm fiber-coupled laser diode which had a core diameter of 400 μm and a numerical aperture of 0.22. The pump beam was focused into the crystal with a radius of 160 μm by a 1 : 0.8 optical collimation system. With the ABCD matrix propagation theory,[17,18] the laser beam inside the gain medium was calculated to be 158 μm in radius, which perfectly matched with the pump light. The Nd:LaGGG crystal employed in our experiment was grown by Czochralski technique with a Nd^{3+} doping level of 1 at% and a La^{3+} doping level of 1.6 at%, which was cut along $\langle 111 \rangle$ direction with dimensions of $4 \times 4 \times 5$ mm^3. It was wrapped with indium foil and tightly mounted in a copper block cooled to be 18 °C. To eliminate Fabry–Perot etalon effect, the crystal was tilted with a small angle with respect to the cavity axis. M1 was a flat mirror with anti-reflectance (AR) coated at 808 nm on the outside surface, high-reflectance (HR) coated at 1.3 μm and high-transmission (HT) coated at 808 nm on the inside surface. M2 and M4 were folded mirrors with HR coated around 1.3 μm, whose radii were 800 mm and 200 mm. A flat mirror M3 with a transmission of 1% at 1.3 μm was used as the output coupler. In order to suppress the laser oscillation at 1.06 μm, all the mirrors were AR coated at 1.06 μm. The commercial SESAM was designed to operate from 1310 nm to 1380 nm with a modulation depth of 0.6%, a non-saturable loss of 0.4%, a saturation fluence of 90 μJ cm^{-2} and a relaxation time of 1 ps. The laser mode radius focused on the SESAM was calculated to be 22 μm. The pulse trains were recorded by a digital oscilloscope (Tektronics DPO 7104) and an InGaAs fast photo-detector (New focus 1611). The pulse width was measured by commercial non-collinear autocorrelator (APE Pulse Check 150) and the output power was recorded by a power-meter (Coherent Inc. Field MaxII-TO). The optical spectrum was recorded using an optical spectrum analyzer (Yokogawa AQ6370C).

Results and discussions

Fig. 2(a) shows the relationship between the average output power and the absorbed pump power. The threshold absorbed pump p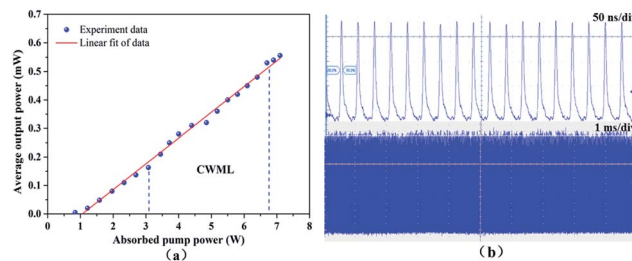ower was 840 mW. It was start operated in the continuous wave regime. Then, as the pump power increased, the Q-switched mode-locking (QML) operation was acquired. After aligning the cavity carefully, especially the distance from M4 to SESAM and the angle of the crystal, simultaneous dual-wavelength continuous-wave mode-locking (CWML) laser centered at 1331.2 nm and 1336.5 nm was obtained when the absorbed pump power exceeded 3.078 W. To achieve stable CWML operation, the intracavity pulse energy should satisfy the theoretical condition[19]

$$E_{P,C} > \sqrt{F_{sat,L} A_L F_{sat,A} A_A \Delta R} \qquad (1)$$

where $E_{P,C}$ is the critical intracavity pulse energy, $F_{sat,L}$ is the saturation fluence of the gain medium, which can be described as $F_{sat,L} = h\nu/(2\sigma_l)$ (σ_l is the emission cross section of the gain medium), $F_{sat,A}$ is the saturation fluence of the SESAM, A_L and A_A are the laser mode areas on the gain medium and SESAM, and ΔR is the modulation depth of the SESAM. The parameters involved in the above formula are listed as follows: $\sigma_l = 4.1 \times 10^{-20}$ cm^2, $F_{sat,A} = 70$ μJ cm^{-2}, $\Delta R = 0.6\%$. The value of $E_{P,C}$ is calculated to be 105 nJ. Experimentally, the intracavity mode-locked single pulse energy was approximately estimated to be 209 nJ with respect to an average output power of 158 mW. When the absorbed pump power was increased to 6.7 W, a maximum average output power of 530 mW was obtained, resulting in the slope efficiency of 9.1% and an optical–optical conversion efficiency of 7.9% and the single pulse energy of 14.09 nJ. The mode-locked pulse trains with a timescale of 50 ns per div and 1 ms per div are shown in Fig. 2(b). It is obvious to see that the laser worked in purely single pulse mode-locking regime. The beam quality factor M^2, was 1.2 and 1.1 in the horizontal and longitudinal planes, respectively, suggesting single transverse mode output.

The optical spectrum of the mode-locked laser is shown in Fig. 3. It was apparent that there were two spectral bands centered at 1331.2 and 1336.5 nm, and the FWHM spectral bandwidths of these two bands were 0.15 and 0.11 nm, respectively. The center frequency difference between the two peaks was determined to be $\Delta\nu = 0.876$ THz. Moreover, the intensity ratio between the two spectral peak signals was 4.5 : 1. From the fluorescence spectrum of Nd:LaGGG crystal as shown as the inset of Fig. 3, we know that there are multiple peaks at 1.3 μm, indicating that Nd:LaGGG laser may operate simultaneously at multiple wavelengths. Three major emission peaks
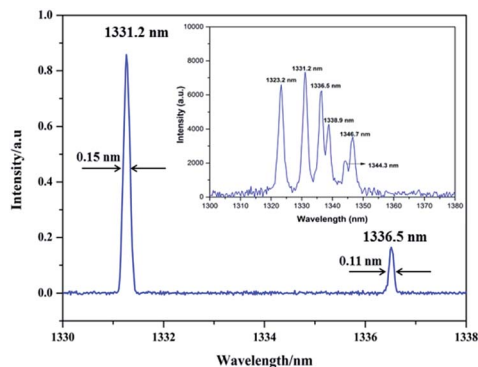
Fig. 3 Optical spectrum of dual-wavelength mode-locked laser. Inset: room-temperature fluorescence spectrum of the transition $^4F_{3/2}$ → $^4I_{13/2}$.[8]

Fig. 5 Autocorrelation trace of the dual-wavelength Nd:LaGGG mode-locked pulses. Inset: the zoom-in measurement of the fine structure.

are centered at 1323.2, 1331.2 and 1336.5 nm. In the experiment, the mode centered at 1323.2 nm couldn't oscillate in this cavity due to the high loss caused by the mirror coating and spectral reflectance of SESAM. High loss centered 1323.2 nm and strong mode competition between them made it difficult to obtain simultaneous tri-wavelength pulses.

Fig. 4 shows the radio-frequency (RF) spectrum of the mode-locked laser with a nice signal-to-noise ratio of 62 dB, which is recorded by a spectrum analyzer (Agilent N9000A) with RBW of 11 kHz. A sharp RF peak at the fundamental beat is 37.6 MHz, which is in well agreement with the cavity length. It is a powerful evidence to prove that the dual-wavelength mode-locked pulses are clean and in good stability.

Fig. 5 shows the autocorrelation trace of the mode-locked laser, from which frequency beating phenomenon is obviously observed. The mode-locked pulse duration is about 17 ps with a $sech^2$ shape assumed. In order to clarify the character of autocorrelation signal, zoom-in details are shown as the inset part of Fig. 5. The beating signal is found to have a FWHM of ~500 fs in duration and beating period of 1.14 ps, exactly corresponding to a reciprocal of $\Delta\nu$. It is also powerful evidence that the perfect spatial overlapping and synchronization of the dual-wavelength mode-locked pulses are achieved.[20]
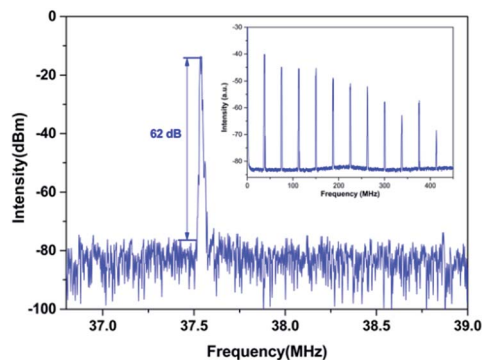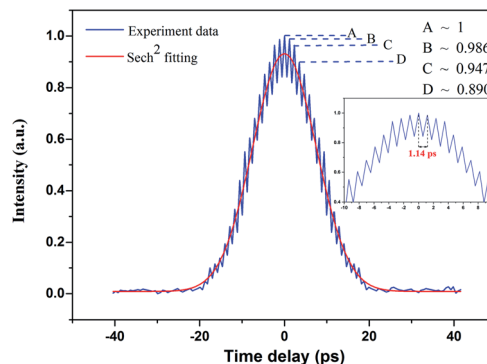
Numerical simulation is conducted to understand the measured autocorrelation trace. The modulation intensity of interference pattern follows this relation[20–22]

$$I = I_1 + I_2 + 2\sqrt{I_1 I_2}\cos(2\pi\Delta\nu t) \qquad (2)$$

where I_1, I_2 and $\Delta\nu$ mean the intensity and the difference frequency of the two wavelengths. According to Fig. 3, the intensity ratio of synchronous dual-color pulses is 4.5 : 1. Using the values, the simulated autocorrelation trace based on eqn (2) is given in Fig. 6. We select the intensity ratio of four points $(A : B : C : D = 1 : 0.987 : 0.949 : 0.889)$ as the comparison value. And the measured major peak intensity ratio of four points is 1 : 0.986 : 0.947 : 0.890 from Fig. 5, which is in fair agreement with the simulated data.

In Table 1, we have collected some results regarding the dual-wavelength synchronously mode-locked lasers reported so far. The derivative of Nd:GGG such as $Nd:Ca_3(NbGa)_2Ca_3O_{12}$ (Nd:CNGG), $Nd:Ca_3Li_{0.20}Ta_{1.88}Ga_{2.80}O_{12}$ (Nd:CLTGG) are the good candidate for dual-wavelength mode-locked lasers due to multiple peaks in fluorescence spectrum caused by the different sites of the Nd ions in the disordered crystal. In addition, among the work of multi-wavelength mode-locked lasers previously reported,[23] the dispersion compensation was necessarily used to synchronize the pulses at different wavelengths. But we did not apply any dispersion compensation
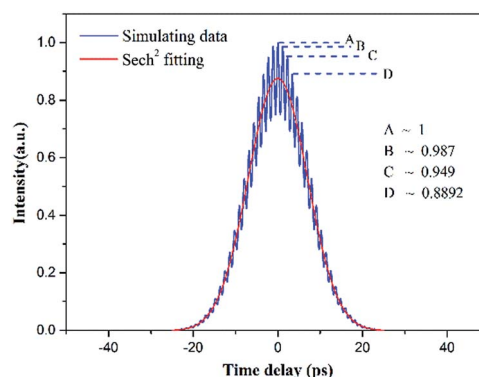

Fig. 4 RF spectrum of the mode-locked laser. Inset: 300 MHz wide-span spectrum with RBW of 1.6 MHz.

Fig. 6 The calculated intensity autocorrelation trace with marks.

Table 1 The dual-wavelength synchronously mode-locked lasers reported so far

Gain medium	Emission wavelength (nm)	Output power (mW)	Pulse width (ps)	Interference beating (THz)	Ref.
Nd:CNGG	1059.1 & 1061.7	90	5	0.63	23
Nd:CLTGG	1059 & 1061	383	3.5	0.53	24
Tm:CaYAlO$_4$	1958.9 & 1960.6	830	35.3	0.13	25
Nd:YAG	1064 & 1123	2470	50.8	14.7	26
Nd:LaGGG	1331.2 & 1336.5	530	17	0.876	This work

components, when stationary modulation patterns were observed. We believe this could be possible because of the saturable absorption of the SESAM, which will produce a kind of attractive force between the pulses.[27] The special force ensures that the dual-color mode-locked pulses have the same cavity roundtrip time and sustains the synchronization of the dual-color pulses for a long time. In fact, it is quite a complex procedure to sustain synchronous mode locking.[28] Many factors such as the spectral separation, the relationship of the gain and loss of the cavity and the intracavity power density contributed to pulse overlap.

Conclusion

In conclusion, a dual-wavelength synchronously continues-wave mode-locking (CWML) Nd:LaGGG laser at 1.3 μm was demonstrated for the first time. An output power of 530 mW was obtained at 6.7 W absorbed pump power with a slope efficiency of 9.1%. The dual-wavelength mode-locked laser was centered at 1331.2 and 1336.5 nm. Without dispersion compensation employed, the measured pulse duration was 17 ps and the beating period is 1.14 ps. A stationary interference pattern was found to have a repetition rate of 0.876 THz. Our results indicated that the Nd:LaGGG crystal was a good candidate for generating dual-wavelength mode-locked pulses.

Acknowledgements

References

1 R. Moncorgé, B. Chambona, J. Y. Rivoirea, N. Garnierb, E. Descroixb, P. Laporteb, H. Guilletc, S. Royc, J. Mareschald, D. Pelencd, J. Dourye and P. Farge, Nd doped crystals for medical laser applications, *Opt. Mater.*, 1997, **8**, 109–119.

2 H. Y. Shen, R. R. Zeng and Y. P. Zhou, Comparison of simultaneous multiple wavelength lasing in various neodymium host crystals at transitions from $^4F_{3/2}$–$^4I_{11/2}$ and $^4F_{3/2}$–$^4I_{13/2}$, *Appl. Phys. Lett.*, 2000, **56**, 1937–1938.

3 L. T. Feng, J. K. Yang, Q. G. Li, S. Z. Zhao, D. C. Li, T. Li, W. C. Qiao, C. Liu, X. Chen, X. D. Xu, L. H. Zheng, J. Xu and R. Lan, Passively mode-locked Nd:LuAG laser at 1338 nm, *Opt. Mater. Express*, 2016, **6**, 1–7.

4 U. Keller, K. J. Weingarten, F. X. Kartner, D. Kopf, B. Braun, I. D. Jung, R. Fluck, C. Honninger, N. Matuschek and J. Aus der Au, Semiconductor saturable absorber mirrors (SESAM's) for femtosecond to nanosecond pulse generation in solid-state lasers, *IEEE J. Sel. Top. Quantum Electron.*, 1996, **2**, 435–453.

5 Y. Yang, J. L. Xu, J. L. He, X. Q. Yang, B. Y. Zhang, H. Yang, S. D. Liu and B. T. Zhang, Diode-pumped passively mode-locked Nd: YAG laser at 1338 nm with a semiconductor saturable absorber mirror, *Appl. Opt.*, 2011, **50**, 6713–6716.

6 Y. Yang, X. Q. Yang, Z. T. Jia, J. L. Xu, J. L. He, S. D. Liu, B. T. Zhang and H. Yang, Diode-pumped passively mode-locked Nd: GGG laser at 1331.3 nm, *Laser Phys. Lett.*, 2012, **9**, 481–484.

7 Z. T. Jia, X. T. Tao, C. Dong, X. Cheng, W. Zhang, F. Xu and M. Jiang, Study on crystal growth of large size Nd^{3+}:Gd$_3$Ga$_5$O$_{12}$ (Nd^{3+}: GGG) by Czochralski method, *J. Cryst. Growth*, 2006, **292**, 386–390.

8 B. Xu, Y. Wang, Y. J. Cheng, H. Y. Xu, Z. P. Cai and R. Moncorgé, Single- and multi-wavelength laser operation of a diode-pumped Nd:GGG single crystal around 1.33 μm, *Opt. Commun.*, 2015, **345**, 111–115.

9 X. W. Fu, Z. T. Jia, Y. B. Li, D. S. Yuan, C. M. Dong and X. T. Tao, Crystal growth and characterization of Nd^{3+}:(La$_x$Gd$_{1-x}$)$_3$Ga$_5$O$_{12}$ laser crystal, *Opt. Mater. Express*, 2012, **2**, 1242–1253.

10 B. Cockayne, D. Gasson, D. Findlay, D. Goodwin and R. Clay, The growth and laser characteristics of yttrium–gadolinium–aluminium garnet single crystals, *J. Phys. Chem. Solids*, 1968, **29**, 905–910.

11 Z. T. Jia, Y. R. Yin, H. Yang, B. T. Zhang, J. L. He, M. Tonelli and X. T. Tao, Highly efficient Nd: (La$_x$Gd$_{1-x}$)$_3$Ga$_5$O$_{12}$ laser operation at 1.33 μm, *Chin. Opt. Lett.*, 2016, **14**, 021405.

12 M. D. Pelusi, H. F. Liu, D. Novak and Y. Ogawa, THz optical beat frequency generation from a single mode-locked semiconductor laser, *Appl. Phys. Lett.*, 1997, **71**, 449–451.

13 C. J. Zhu, J. F. He and S. C. Wang, Generation of synchronized femtosecond and picosecond pulses in a dual-wavelength femtosecond Ti:sapphire laser, *Opt. Lett.*, 2005, **30**, 561–563.

14 J. M. Evans, D. E. Spence, D. Burns and W. Sibbett, Dual-wavelength self-mode-locked Ti:sapphire laser, *Opt. Lett.*, 1993, **18**, 1074–1076.

15 M. D. Pelusi, H. F. Liu, D. Novak and Y. Ogawa, THz optical beat frequency generation from a single mode-locked semiconductor laser, *Appl. Phys. Lett.*, 1997, **71**, 449.

16 J. Sun, Y. T. Dai, X. F. Chen, Y. J. Zhang and S. Z. Xie, Stable Dual-Wavelength DFB Fiber Laser With Separate Resonant Cavities and Its Application in Tunable Microwave Generation, *IEEE Photonics Technol. Lett.*, 2005, **18**, 2587–2589.

17 V. Magni, G. Cerullo and S. D. Silvestri, ABCD matrix analysis of propagation of Gaussian beams through Kerr media, *Opt. Commun.*, 1993, **96**, 348–355.

18 M. Nakazawa, H. Kubota, A. Sahara and K. Tamura, Time-domain ABCD matrix formalism for laser mode-locking and optical pulse transmission, *IEEE J. Sel. Top. Quantum Electron.*, 1998, **34**, 1075–1081.

19 C. Hönninger, R. Paschotta, F. Morier-Genoud, M. Moser and U. Keller, Q-Switching sta bility limits of continuous-wave passive mode locking, *J. Opt. Soc. Am. B*, 1999, **16**, 46–56.

20 C. L. Wang and C. L. Pan, Tunable multiterahertz beat signal generation from a two-wavelength laser-diode array, *Opt. Lett.*, 1995, **20**, 1292–1294.

21 Z. H. Cong, D. Y. Tang, W. D. Tan, J. Zhang, C. W. Xu, D. W. Luo, X. D. Xu, D. Z. Li, J. Xu, X. Y. Zhang and Q. P. Wang, Dual-wavelength passively mode-locked Nd:LuYSiO$_5$ laser with SESAM, *Opt. Express*, 2011, **19**, 3984–3989.

22 J. Hou, L. H. Zheng, J. L. He, J. Xu, B. T. Zhang, Z. W. Wang, F. Lou, R. H. Wang and X. M. Liu, A tri-wavelength synchronous mode-locked Nd: SYSO laser with a semiconductor saturable absorber mirror, *Laser Phys. Lett.*, 2014, **11**, 035803.

23 G. Q. Xie, D. Y. Tang, H. Luo, H. J. Zhang, H. H. Yu, J. Y. Wang, X. T. Tao, M. H. Jiang and L. J. Qian, Dual-wavelength synchronously mode-locked Nd:CNGG laser, *Opt. Lett.*, 2008, **33**, 1872–1874.

24 J. L. Xu, S. Y. Guo, J. L. He, B. Y. Zhang, Y. Yang, H. Yang and S. D. Liu, Dual-wavelength asynchronous and synchronous mode-locked operation by a Nd:CLTGG disordered crystal, *Appl. Phys. B*, 2012, **107**, 53–58.

25 L. C. Kong, Z. P. Qin, G. Q. Xie, X. D. Xu, J. Xu, P. Yuan and L. J. Qian, Dual-wavelength synchronous operation of a mode-locked 2 μm Tm:CaYAlO$_4$ laser, *Opt. Lett.*, 2015, **40**, 356–358.

26 C. L. Sung, C. Y. Lee, C. C. Chang, H. C. Liang and Y. F. Chen, Generation of terahertz optical beating from a simultaneously self-mode-locked Nd:YAG laser at 1064 and 1123 nm, *Opt. Lett.*, 2017, **42**, 302–305.

27 L. M. Zhao, D. Y. Tang and H. Zhang, Bunch of restless vector solitons in a fiber laser with SESAM, *Opt. Express*, 2009, **17**, 8103–8108.

28 L. C. Kong, Z. P. Qin, G. Q. Xie, *et al.*, Dual-wavelength synchronous operation of a mode-locked 2 μm Tm:CaYAlO$_4$ laser, *Opt. Lett.*, 2015, **40**, 356–358.